

# Spectral-Domain Optical Coherence Tomography Angiography of Choroidal Neovascularization

Talisa E. de Carlo, BA,<sup>1,2</sup> Marco A. Bonini Filho, MD, PhD,<sup>1,3</sup> Adam T. Chin, BA,<sup>1</sup> Mehreen Adhi, MD,<sup>1,2</sup> Daniela Ferrara, MD, PhD,<sup>1</sup> Caroline R. Baumal, MD,<sup>1</sup> Andre J. Witkin, MD,<sup>1</sup> Elias Reichel, MD,<sup>1</sup> Jay S. Duker, MD,<sup>1</sup> Nadia K. Waheed, MD, MPH<sup>1</sup>

**Purpose:** To describe the characteristics as well as the sensitivity and specificity of detection of choroidal neovascularization (CNV) on optical coherence tomography angiography (OCTA) using spectral-domain optical coherence tomography.

**Design:** Observational, retrospective study.

**Participants:** Seventy-two eyes of 61 subjects (48 eyes of 43 subjects with CNV, 24 eyes of 18 subjects without CNV).

**Methods:** Patients imaged using the prototype AngioVue OCTA system (Optovue, Inc, Fremont, CA) between August 2014 and October 2014 at New England Eye Center were assessed. Patients in whom CNV was identified on OCTA were evaluated to define characteristics of CNV on OCTA: size using greatest linear dimension (small, <1 mm; medium, 1–2 mm; large, >2 mm), appearance (well-circumscribed, poorly circumscribed), and presence of subretinal and intraretinal fluid. Concurrently, an overlapping second cohort of patients who underwent same-day OCTA and fluorescein angiography (FA) for suspected CNV was evaluated to estimate sensitivity and specificity of OCTA in detecting CNV using FA as ground truth.

**Main Outcome Measures:** Choroidal neovascularization appearance, CNV size, and presence of subretinal and intraretinal fluid.

**Results:** In 48 eyes, CNV was visualized on OCTA. Thirty-one eyes had CNV associated with neovascular age-related macular degeneration. Size of CNV was small in 23% (7/31), medium in 42% (13/31), and large in 35% (11/31). Poorly circumscribed vessels, subretinal fluid, and intraretinal fluid each were seen in 71% (22/31). Seven eyes had CNV associated with central serous chorioretinopathy. Size of CNV was small in 71% (5/7) and large in 29% (2/7). Seventy-one percent (5/7) had well-circumscribed vessels, 86% (6/7) had subretinal fluid, and 14% (1/7) had intraretinal fluid. Thirty eyes with OCTA and same-day FA were evaluated to determine sensitivity and specificity of CNV detection on OCTA. Sensitivity was 50% (4/8) and specificity was 91% (20/22).

**Conclusions:** Using OCTA allows the clinician to visualize CNV noninvasively and may provide a method for identifying and guiding treatment of CNV. The specificity of CNV detection on OCTA compared with FA seems to be high. Future studies with larger sample sizes are needed to elaborate better on the sensitivity and specificity of CNV detection and to illustrate clinical usefulness. *Ophthalmology* 2015;■:1–11 © 2015 by the American Academy of Ophthalmology.

Choroidal neovascularization (CNV) can occur as a result of a variety of ophthalmologic diseases, such as neovascular age-related macular degeneration (AMD), high myopia, central serous chorioretinopathy (CSCR), multifocal choroiditis, and others. These abnormal blood vessels typically are derived from the choroidal vasculature and can penetrate Bruch's membrane into the space beneath the retinal pigment epithelium (RPE; type 1 CNV) or the subretinal space (type 2 CNV). In some eyes, neovascularization seems to begin from the retinal vasculature, eventually anastomosing with new vessels derived from the choroidal vasculature (retinal angiomatous proliferation, also called type 3 CNV).<sup>1–3</sup> Early diagnosis and visualization of CNV are crucial for initiating and guiding treatment, which in most cases is an intravitreal

anti-vascular endothelial growth factor (VEGF) drug to prevent progressive, irreversible vision loss.<sup>4</sup>

The current gold standard for identifying CNV is fluorescein angiography (FA).<sup>5–7</sup> Fluorescein angiography uses intravenous dye injection to visualize CNV, and the patterns of hyperfluorescence that accompany the various kinds of CNV have been well characterized.<sup>8–10</sup> Although considered safe, intravenous dye has risks ranging from discomfort and nausea to, in rare cases, anaphylaxis. Fluorescein angiography is not considered an appropriate screening test for CNV detection in an asymptomatic population. In addition, the technique is expensive and time consuming, requiring up to 10 minutes of imaging time, which can limit its routine use in a busy clinical setting.<sup>11,12</sup>

For these reasons, a noninvasive imaging technique to detect rapidly and to monitor CNV without the use of intravenous dye is desirable. Optical coherence tomography (OCT) has become an important noninvasive method for structural imaging of patients with suspected CNV. It enables visualization of subretinal fluid, intraretinal fluid, retinal pigment epithelial detachments (RPEDs), and retinal thickening using cross-sectional B-scans. Choroidal neovascularization may appear on structural OCT B-scans as subretinal or sub-RPE hyperreflective material, or both, often with breaks in Bruch's membrane and interruption of the RPE, but differentiation between fibrous and vascular tissue is limited using cross-sectional scans. In type 1 CNV, structural en face OCT images using enhanced depth imaging (EDI) may successfully visualize the branching CNV network below the RPE. However, this method is limited to use in fibrovascular RPEDs and therefore is not widely applicable to all types of CNV.<sup>13</sup> Thus, at the present time, there are no agreed-on standards for diagnosing CNV based strictly on cross-sectional OCT. Structural OCT cannot detect blood flow, nor can it reliably distinguish vasculature from fibrous and other surrounding tissue.<sup>4</sup> Therefore, OCT findings are used in conjunction with leakage on FA to diagnose CNV definitively.<sup>14–16</sup>

Optical coherence tomography angiography (OCTA) allows noninvasive visualization of retinal and choroidal vasculature via motion contrast imaging. This relatively new imaging technique maps erythrocyte movement over time by comparing sequential OCT B-scans at a given crosssection. Motion correction technology removes axial bulk motion from patient movement so that regions of motion between repeated OCT B-scans correspond to erythrocyte flow and, therefore, vasculature. Compared with structural OCT images, higher imaging speeds are required to obtain a densely sampled volume on OCTA. Conventional scanning speeds would result in decreased quality (because of undersampling), decreased field of view, increased acquisition time, or a combination thereof. Optical coherence tomography angiograms are coregistered with OCT B-scans from the same area, allowing for simultaneous visualization of structure and blood flow.<sup>17–19</sup> Jia et al<sup>4</sup> described a technique that uses a prototype swept-source (SS) OCT to visualize CNV noninvasively via OCTA, using the split-spectrum amplitude decorrelation angiography (SSADA) algorithm to improve flow detection and improve CNV visualization. To our knowledge, no group has studied CNV using a commercially available spectral-domain (SD) OCT. This study used an OCTA system based on a commercially available SD OCT device (Optovue, Inc., Fremont, CA), using a prototype OCTA SSADA algorithm to visualize CNV using noninvasive OCTA.

## Methods

This study was approved by the institutional review board of Tufts Medical Center. Informed consent was obtained from patients in accordance with the Tufts Medical Center Institutional Review Board before examination. The research adhered to the tenets of the Declaration of Helsinki and complied with the Health Insurance

Portability and Accountability Act of 1996. In this retrospective review, patients who underwent OCTA using the prototype AngioVue OCTA system on the commercially available Avanti SD OCT device (Optovue, Inc) between August 2014 and October 2014 at the Retina Service of the New England Eye Center at Tufts Medical Center were evaluated.

The AngioVue OCTA system used an SSADA software algorithm and operated at 70 000 A-scans per second to acquire OCTA volumes consisting of 304×304 A-scans in approximately 2.6 seconds. Orthogonal registration and merging of 2 consecutive scan volumes were used to obtain 3×3-mm and 6×6-mm OCTA volumes of both eyes of each patient. Both 3×3-mm and 6×6-mm OCTA volumes used a 304×304 scanning pattern. Optical coherence tomography angiograms were coregistered with the OCT B-scans obtained concurrently, allowing visualization of both retinal flow and structure in tandem. In addition, the SD OCT device was capable of acquiring the standard structural OCT scans typically used by commercially available devices in the evaluation of CNV (i.e., high-resolution line scans and cube scans).

The OCTA software was used to delineate a region of interest with an inner border at the level of the outer aspect of the inner nuclear layer (seen as a green line on the corresponding OCT B-scan) and an outer border at the level of Bruch's membrane (shown as a red line on the corresponding OCT B-scan). An artifact removal toggle function within the software was used to remove retinal vessel shadowing from the en face flow image. This function worked by automatically subtracting vessels that were seen above the inner border (vasculature of the inner retina) from the outer retina OCTA image. Therefore, only vessels truly within the outer retina segmentation boundary were shown. In healthy individuals, the outer retina is not expected to have blood vessels. Therefore, after accurate segmentation and retinal vessel shadowing removal, vessels identified in this region were presumed to be neovascularization. The levels of the inner and outer boundaries determining the thickness of the en face (C scan) section were fine-tuned manually to include all of the area suspicious for CNV as visualized on the corresponding OCT B-scan images. The inner boundary was adjusted to contain the innermost region suspicious of a CNV (characterized by disruption of the RPE, presence of subretinal fluid, RPED, or subretinal hyperreflective material). The outer boundary was adjusted to lie directly anterior to Bruch's membrane so minimal choroidal vasculature would be included in the region being imaged by OCTA. The prototype software did not allow the segmentation curve of the inner or outer limits to be adjusted; it only allowed movements up or down using the original automated segmentation line course, which was calculated automatically based on the contour of Bruch's membrane.

The 3×3-mm OCTA images were used primarily to evaluate each eye. If a 3×3-mm OCTA image did not show a CNV, the findings were confirmed by evaluating the 6×6-mm OCTA image to ensure that more peripheral CNVs were not missed. In cases where the 3×3-mm OCTA image showed a CNV that extended beyond the image border, a 6×6-mm OCTA image was used so that the entire CNV was evaluated.

All patients in whom CNV was identified on OCTA underwent further review of the medical records for patient characteristics and underlying diagnosis. The OCTAs were evaluated independently by 2 trained readers (T.E.D., M.A.B.F.) from the Boston Image Reading Center, Tufts Medical Center, to confirm the diagnosis and to define the characteristics of the CNV identified on the OCTA. The OCTA images and coregistered corresponding OCT B-scans were assessed for CNV size, CNV appearance, and presence of subretinal fluid, intraretinal fluid, and RPED. The CNV size was classified on the OCTA image as follows: small if the greatest linear dimension (GLD) was less than 1 mm, medium if GLD was between 1 and 2 mm, and

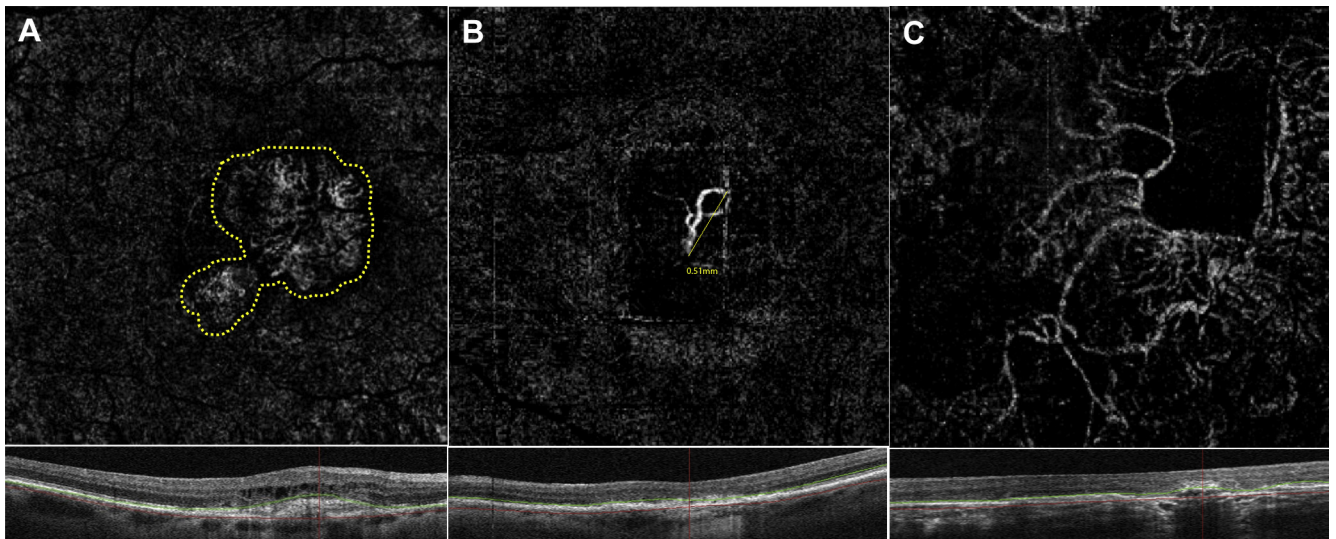


**Figure 1.** Optical coherence tomography angiography (OCTA) images showing the grading schema. **A**, A 3×3-mm and corresponding optical coherence tomography (OCT) B-scan showing a medium, well-circumscribed choroidal neovascularization (CNV). **B**, A 3×3-mm OCTA image and corresponding OCT B-scan of a small, filamentous CNV determined by measurement of the greatest linear dimension. **C**, A 3×3-mm OCTA image and corresponding OCT B-scan of a large, poorly circumscribed, filamentous CNV.

large if the GLD was more than 2 mm. Appearance of CNV on the OCTA image was classified as well circumscribed (typically sea fan-shaped vessels) or poorly circumscribed (long filamentous vessels). Subretinal fluid and intraretinal fluid were determined to be present or absent using the correlating OCT B-scans. [Figure 1](#) illustrates examples of the grading schema. In the cases where follow-up OCTA images were obtained on the eye, only the first OCTA of each eye was included in the results.

Concurrently, an overlapping smaller cohort of patients was evaluated to estimate the sensitivity and specificity of OCTA compared with FA. This second group of eyes did not have a confirmed clinical diagnosis of CNV and all underwent same-day FA for suspicion of CNV. The OCTAs of these patients were assessed by 2 trained readers (T.E.D., M.A.B.F.) at the Boston Image Reading Center for presence or absence of CNV. Similarly, the same-day FAs of all of these patients were evaluated independently from the OCTAs

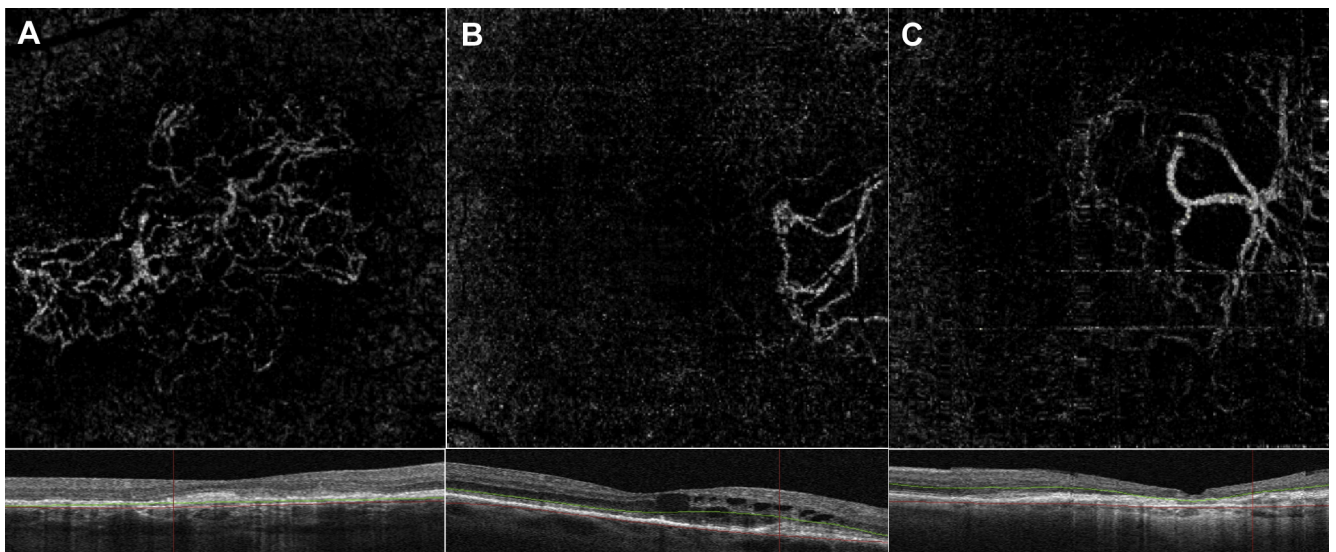


**Figure 2.** Optical coherence tomography angiography (OCTA) images showing case examples of choroidal neovascularization (CNV) and subretinal fluid. **A**, A 3×3-mm OCTA image and correlating optical coherence tomography (OCT) B-scan image of a 68-year-old white woman with central serous chorioretinopathy showing a large CNV with long curving vessels on OCTA image, but no subretinal or intraretinal fluid on correlating OCT B-scan. **B**, A 3×3-mm OCTA image and correlating OCT B-scan image of an 84-year-old white woman with neovascular age-related macular degeneration (AMD) showing a medium CNV with long filamentous vessels on the OCTA image. On the associated OCT B-scan, a retinal pigment epithelial detachment and intraretinal fluid are apparent. **C**, A 3×3-mm OCTA image and correlating OCT B-scan image of an 87-year-old white woman with neovascular AMD showing clearly demarcated thin filamentary vessels on the OCTA image, but no subretinal fluid on the correlating OCT B-scan.

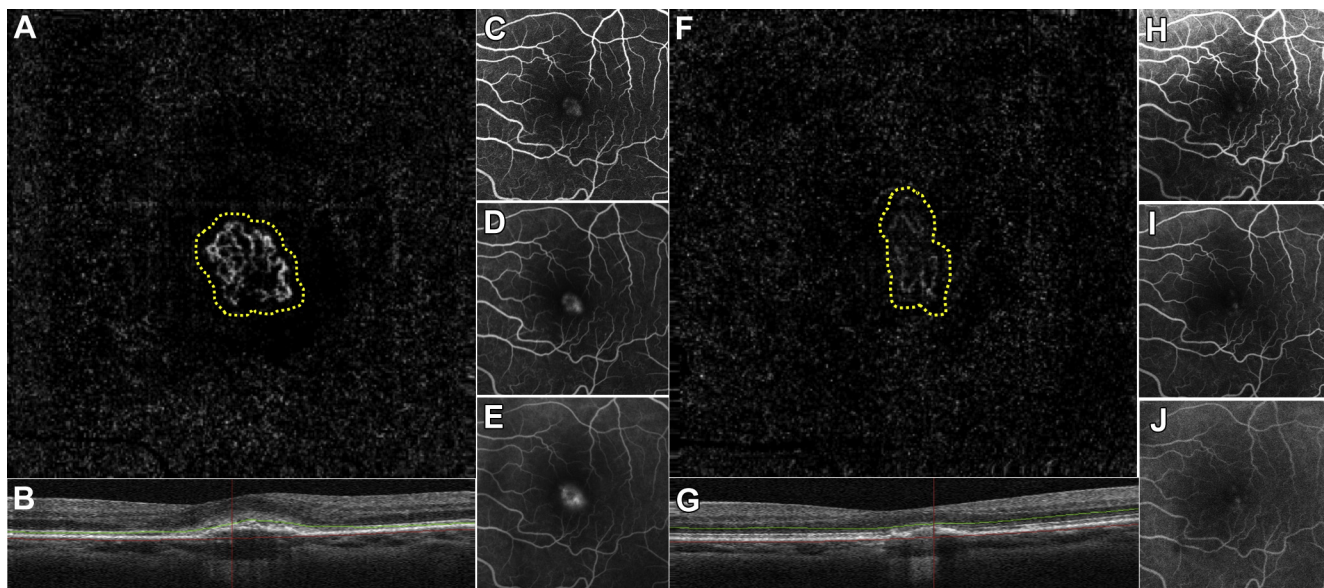


**Figure 3.** Choroidal neovascularization (CNV) on optical coherence tomography angiography (OCTA) images and FA at first visit, then CNV seen on OCTA, but not fluorescein angiography (FA), on follow-up visit. **A**, A 3×3-mm OCTA image from a 47-year-old Asian woman with multifocal choroiditis showing CNV at the macula. **B**, Correlating OCT B-scan showing a retinal pigment epithelial detachment concerning for CNV. **C**, Early-frame FA image from the patient in Figure 3A showing hyperfluorescence in the region of CNV. **D**, Intermediate-frame FA image of the patient in Figure 3A showing increasing CNV hyperfluorescence. **E**, Late-frame FA image of the patient in Figure 3A showing pooling. **F**, A 3×3-mm OCTA image of the same 47-year-old Asian woman with multifocal choroiditis 2 months after intravitreal anti-vascular endothelial growth factor injection showing the CNV is still present, but decreased in size. **G**, Correlating OCT B-scan showing that the retinal pigment epithelial detachment concerning for CNV has decreased in size horizontally. Of note, the vertical dimension of the CNV appears larger possibly because of neovascular growth in this area. **H–J**, Early-, intermediate-, and late-frame FA images of the patient from the same follow-up visit in Figure 3F showing mild hyperfluorescence that is stable throughout the FA in the region of CNV without pooling.

for presence or absence of CNV. Fluorescein angiography then was used as the ground truth to calculate the sensitivity and specificity of OCTA in visualizing CNV. If an eye was determined to have CNV on FA, the OCTA image was considered a true positive if a CNV was seen or a false negative if the CNV was not visualized. If the FA did not demonstrate a CNV, the OCTA image was considered a true negative if no CNV was seen or a false positive if a CNV was considered present. In 3 cases where same-day FA and OCTA images were obtained in an eye on multiple visits, only the first OCTA and FA were used in the calculations. Same-day reflectance en face OCT images also were evaluated in this cohort for presence or absence of CNV to see how OCTA compared with en face OCT in visualizing CNV.

## Results

Choroidal neovascularization was visualized on OCTA in 48 eyes of 43 subjects. Six of these eyes of 6 patients also were reviewed in the overlapping cohort in which same-day FA and OCTA were evaluated for sensitivity and specificity calculations. Including these 6 eyes, the cohort contained 30 eyes of 24 subjects. Therefore, in total, this study included 72 eyes from 61 subjects. All eyes evaluated in this study demonstrated agreement between 3×3-mm and 6×6-mm OCTA images.

Forty-eight eyes of 43 patients were presumed to have CNV based on OCTA. Patient ages ranged from 24 to 99 years, with a mean of 69 years. Forty patients were white, 2 patients were Asian, and 1 patient was Hispanic. There were 28 women and 15 men included. Of the 48 eyes, 31 had neovascular AMD, 7 had CSCR, and 10 had a different diagnosis (angioid streaks, multifocal

choroiditis, myopic degeneration, pars planitis, or an unclear diagnosis with the differential diagnosis including CSCR, neovascular AMD, or polypoidal choroidal vasculopathy). Ten of these eyes underwent OCTA twice on different dates (an initial and a follow-up examination), 2 eyes underwent follow-up OCTA twice, and 1 eye underwent follow-up OCTA 3 times.

All 48 eyes had an RPED in the region of CNV identified on the OCTA's correlating OCT B-scan. In the 31 eyes with CNV associated with neovascular AMD, CNV size was distributed as follows: 23% (7/31) were small, 42% (13/31) were medium, and 35% (11/31) were large. Poorly circumscribed vessels were observed in 71% (22/31) of eyes on the OCTA images; 71% (22/31) of eyes had subretinal fluid and 71% (22/31) of eyes had intraretinal fluid on the correlating OCT B-scans. Of the 7 eyes with CNV associated with CSCR, CNV was well circumscribed in 71% (5/7), small in 71% (5/7), medium in 0% (0/7), and large in 29% (2/7) of eyes on the OCTA images. Subretinal fluid was seen in 86% (6/7) of the CSCR OCT B-scans, but intraretinal fluid was seen in only 14% (1/7). Of the 10 eyes with CNV associated with diagnoses other than AMD or an indeterminate diagnosis, 60% (6/10) of the CNVs were well circumscribed, 50% (5/10) were small, 20% (2/10) were medium, and 30% (3/10) were large on the OCTA images. Concurrent subretinal fluid and intraretinal fluid were seen on the correlating OCT B-scans in 60% (6/10) and 70% (7/10), respectively.

Figure 2 demonstrates 3 OCTA images. Figure 2A is from a 68-year-old white woman with CSCR showing a large CNV with long filamentous vessels on the OCTA image, but no subretinal or intraretinal fluid on correlating OCT B-scan. Figure 2B is from an 84-year-old white woman with neovascular AMD demonstrating a medium CNV with long filamentous vessels on the OCTA image. On the associated OCT B-scan, an RPED and intraretinal fluid are

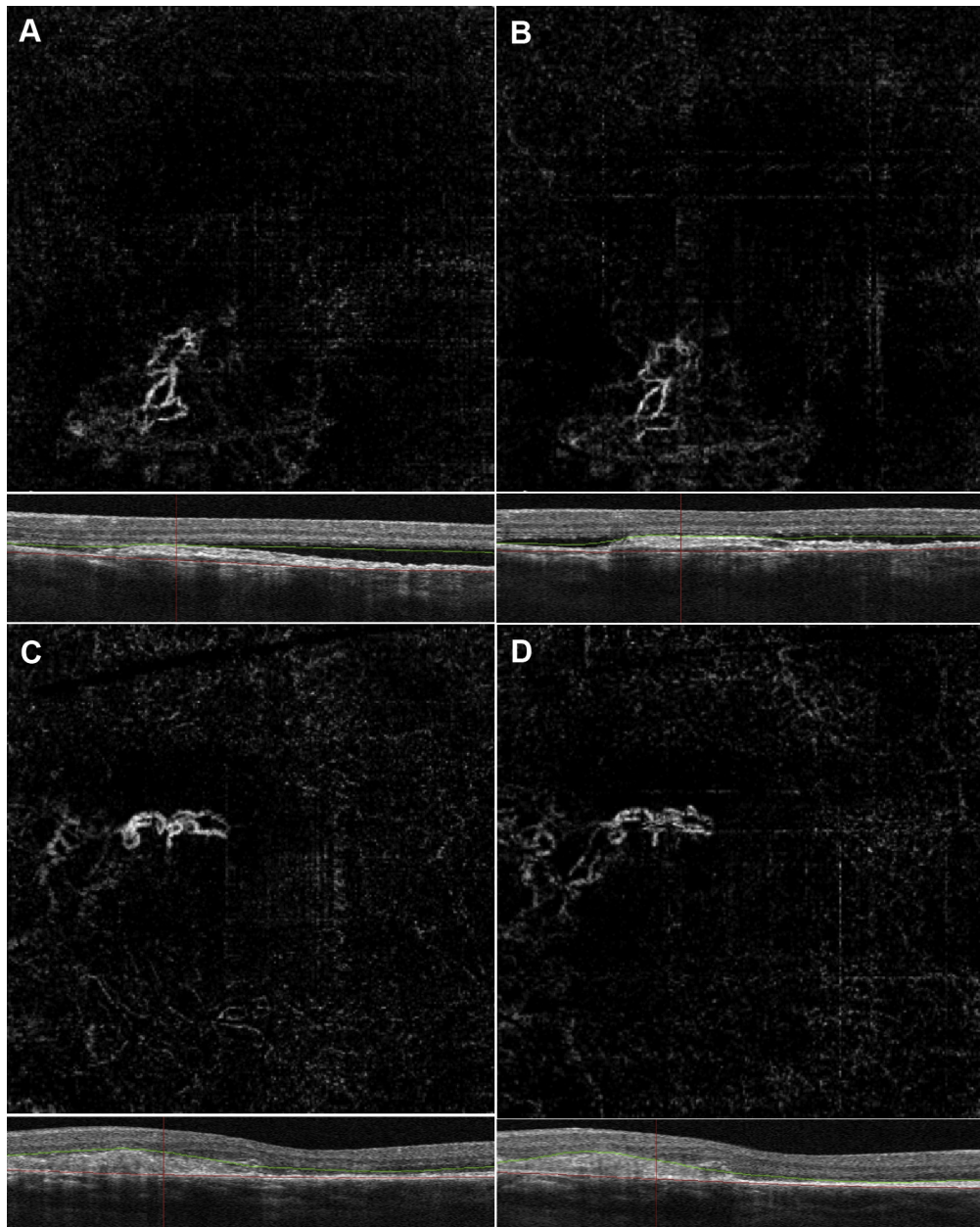


**Figure 4.** Longitudinal visualization of choroidal neovascularization (CNV) shown on  $3\times 3$ -mm optical coherence tomography angiography (OCTA) images and correlating optical coherence tomography (OCT) B-scans. **A**, A 62-year-old white woman with central serous chorioretinopathy. **B**, Same patient in Figure 4A 5 weeks after intravitreal injection of anti-vascular endothelial growth factor, showing no notable change in CNV or subretinal fluid. **C**, A 56-year-old man with neovascular age-related macular degeneration. **D**, Same patient in Figure 4C showing possible minimal CNV growth 2 weeks later after observation.

apparent. [Figure 2C](#) illustrates a clearly demarcated thin filamentary CNV on the OCTA image of an 87-year-old white woman with neovascular AMD, but no subretinal or intraretinal fluid on correlating OCT B-scan.

Thirteen eyes with CNV had follow-up OCTA. Of these, all 13 eyes (100%) had CNV seen on every OCTA date. Follow-up OCTA showed image consistency and allowed for monitoring of changes in size and fluid. One of the patients, a 47-year-old woman, showed sequential reduction in the size of CNV 1 week, 3 weeks, and 2 months after injection with anti-VEGF ([Fig 3](#)). A 62-year-old white woman with CNV secondary to CSCR

showed no change in OCTA 5 weeks after an intravitreal anti-VEGF injection. A third patient, a 56-year-old white man, demonstrated consistent CNV size on OCTA after 2 weeks of observation ([Fig 4](#)).

All patients who underwent OCTA and FA for suspected CNV on the same date of service between August 2014 and October 2014 were evaluated in an overlapping second cohort. Thirty eyes of 24 patients were assessed. Patient ages ranged from 29 to 91 years (mean, 64 years). There were 19 white patients and 5 Asian patients, and 12 patients were men and 12 patients were women. Of the 30 eyes assessed, 8 eyes clearly demonstrated CNV on FA as

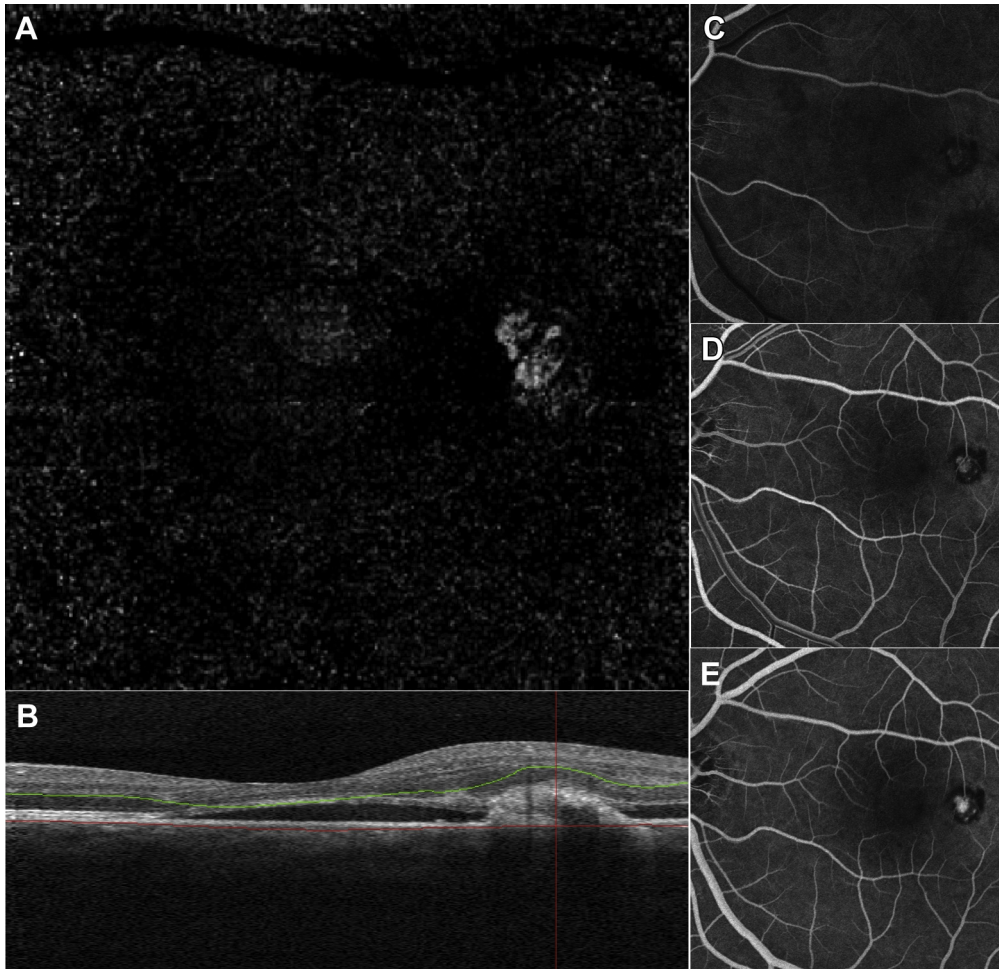


**Figure 5.** Choroidal neovascularization (CNV) on optical coherence tomography angiography (OCTA) images and fluorescein angiography (FA) images. **A**, A 3×3-mm OCTA image from a 31-year-old white man with central serous chorioretinopathy and secondary CNV showing a small well-circumscribed CNV temporal to the macula surrounded by a halo of choriocapillaris vessels. **B**, Correlating optical coherence tomography B-scan of the patient in Figure 5A showing subretinal fluid and a retinal pigment epithelial detachment concerning for CNV. **C**, Early-frame FA image from the patient in Figure 5A showing hyperfluorescence in the region of CNV. **D**, Intermediate-frame FA image from the patient in Figure 5A showing increasing CNV hyperfluorescence. **E**, Late-frame FA image of the patient in Figure 5A showing leakage and pooling.

established by an independent evaluation by 2 trained readers at the Boston Image Reading Center, whereas CNV was determined to be absent in the other 22 FAs. Of the 8 images with CNV detected by FA, 4 also were detected to have CNV using OCTA. Sensitivity of CNV detection by OCTA therefore was 50%. Of the 22 images without CNV on FA, 20 also were determined to have no CNV on OCTA. Specificity of CNV detection by OCTA thus was 91%. No CNV could be detected unequivocally on any of the 30 eyes using reflectance en face OCT.

Figure 5 shows OCTA and FA images from a 31-year-old white man with long-standing CSCR and a question of secondary CNV in the left eye. The FA image demonstrates the presence of a CNV temporal to the macula, showing hyperfluorescence early with later leakage in the region of CNV. The OCTA image also illustrates a small, well-circumscribed CNV temporal to the fovea.

Figure 6 shows FA and OCTA images from a 60-year-old white woman with multifocal choroiditis. The FA was considered questionable for CNV by the clinician (N.K.W.) evaluating the patient. However, upon formal reading by the Boston Image Reading Center, the FA ultimately was determined to show positive results

for CNV because of stippled hyperfluorescence in the intermediate frame followed by late pooling. However, CNV clearly was evident on the OCTA image in the superior-nasal macula.

Figure 3 demonstrates 2 visits of a 47-year-old Asian woman with multifocal choroiditis; the patient underwent FA and OCTA at each visit. The patient had treatment-naïve CNV at the first visit. At that time, FA and OCTA both showed the CNV clearly. Two months later, after intravitreal anti-VEGF injection, the patient had a smaller but still notable CNV in the outer retina segmentation of the OCTA but no apparent CNV on FA. As can be seen on the OCTA images, the patient still had apparently perfused vessels that did not leak on the FA.

## Discussion

Jia et al<sup>4</sup> reported 5 cases of CNV and compared them with normal eyes using OCTA from a prototype SS OCT and hinted at the potential future usefulness of OCTA in

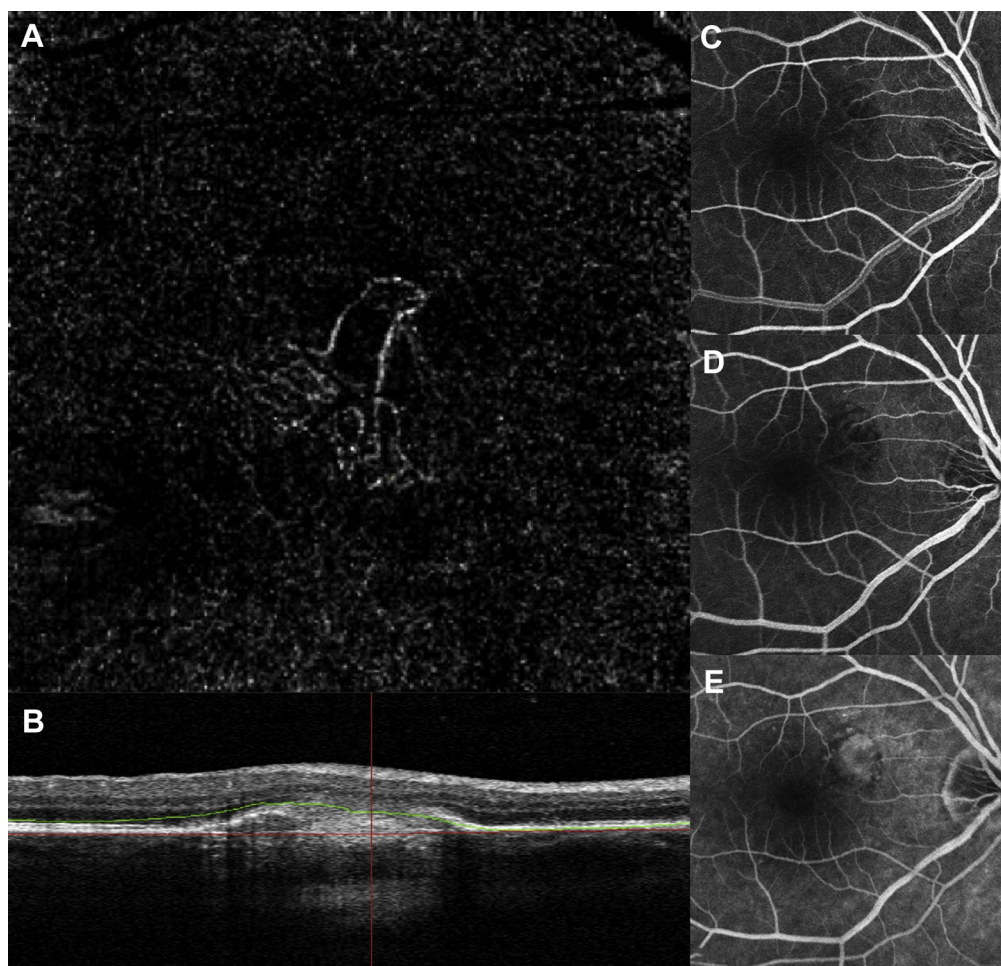


**Figure 6.** Choroidal neovascularization (CNV) on optical coherence tomography angiography (OCTA) images and fluorescein angiography (FA) images. **A**, A 3×3-mm OCTA from a 60-year-old white woman with multifocal choroiditis showing a CNV in the superonasal macula. **B**, Correlating optical coherence tomography B-scan of the patient in Figure 6A showing a retinal pigment epithelial detachment concerning for CNV. **C**, Early-frame FA image from the patient in Figure 6A without clear hyperfluorescence. **D**, Intermediate-frame FA image from the patient in Figure 6A showing stippled hyperfluorescence. **E**, Late-frame FA image from the patient in Figure 6A showing pooling.

quantifying CNV. Their prototype system operated at 100 000 A-scans per second to acquire 200×200 A-scans in 3.5 seconds. Orthogonal registration and merging of 4 scans then were used to create 3×3-mm OCTA images. The series presented in this manuscript is a larger qualitative and quantitative study that investigated OCTA imaging using the AngioVue OCTA system using a commercially available SD OCT engine. The AngioVue system operates at 70 000 A-scans per second to obtain 304×304 A-scans in 2.6 seconds, merging and registering 2 consecutive scans to achieve 3×3-mm or 6×6-mm OCTA images. This study demonstrated the usefulness of the AngioVue system based on application of an SSADA to data acquired from a commercially available SD OCT system, which used decreased scanning speeds, but fewer repeated B-scans, and therefore faster imaging time than the SS OCT prototype. The AngioVue system was useful in localizing and measuring the size of the CNV.

Fluorescein angiography remains the current gold standard for diagnosing CNV. However, FA is invasive, is time

consuming, provides only a 2-dimensional image, and has a low but significant risk profile that includes nausea, allergy, and, rarely, anaphylaxis.<sup>5–7</sup> Optical coherence tomography angiography is a noninvasive, depth-resolved, rapid technique for imaging CNV. Optical coherence tomography angiography was capable of visualizing CNV via semi-automated segmentation of the outer retina and subretinal or sub-RPE space from a volumetric SD OCT dataset. Moreover, corresponding OCT B-scans obtained concurrently were useful for identifying subretinal fluid and other anatomic nonvascular features that also were relevant in the diagnosis of CNV and disease activity.

Sensitivity and specificity of CNV detection by OCTA were 50% and 91%, respectively, in our study. The 2 cases classified in this study as showing false-positive results had clearly perfused vessels on OCTA, but the FA images were interpreted as showing negative results. It is intriguing to contemplate whether the presence of vessels such as these on OCTA after treatment could represent persistent CNV that is not actively leaking on FA but could have

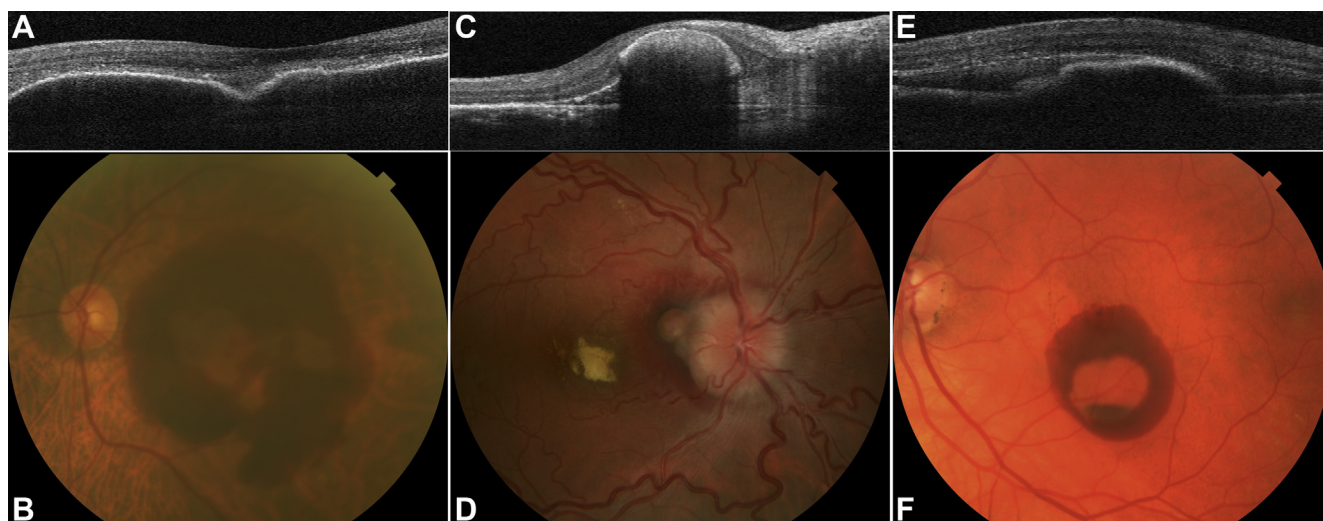


**Figure 7.** Images of subretinal hemorrhage observed in false-negative cases. **A**, A 3-mm optical coherence tomography angiography (OCTA) image correlating B-scan showing large amounts of subretinal hemorrhage over the retinal pigment epithelial (RPE) detachment. **B**, Color fundus photograph of the patient in Figure 7A displaying large amounts of subretinal hemorrhage. **C**, A 3-mm OCTA correlating B-scan demonstrating large amounts of subretinal hemorrhage over the suspicious peripapillary lesion. **D**, Color fundus photograph of the patient in Figure 7C showing large amounts of peripapillary subretinal hemorrhage. **E**, A 3-mm OCTA correlating B-scan displaying large amounts of subretinal hemorrhage over the RPE detachment. **F**, Color fundus photograph from the patient in Figure 7E demonstrating large amounts of subretinal hemorrhage.

implications regarding the recurrence of CNV. Further longitudinal studies would be needed to evaluate better this hypothesis. Upon review of the 4 false-negative cases, 3 of the 4 OCTA images had a large amount of subretinal hemorrhage (Fig 7). Because the OCT signal is blocked by the presence of hemorrhage, OCTA may not be ideal for the diagnosis of CNV in these patients. The increased penetrance of an SS OCT system or an OCTA EDI protocol may be an advantage for CNV visualization. Further head-to-head comparative studies are needed to confirm this. Additionally, when the same 3 OCTA images were reevaluated in a nonblinded fashion in conjunction with the corresponding OCT B-scans and the known CNV location as determined by the FA, it was possible to appreciate indistinct areas of so-called flow on the OCTA images. These areas had not been identified as CNV by the 2 readers because they did not have identifiable vessel contours and therefore resembled surrounding areas of noise. Using multimethod imaging in this fashion, after the CNV was identified on OCTA, may allow the CNV to be observed noninvasively over time for growth, regression, and recurrence. Therefore, although OCTA did not have increased initial sensitivity as a stand-alone method in this situation, it would make monitoring of CNV over time easier.

The fourth of the 4 false-negative OCTA images contained a lesion in the innermost outer retina that was highly debated by the Boston Image Reading Center readers because of large amounts of motion artifact. The final read was that the eye likely contained a retinal angiomatous proliferation lesion, not a type 1 or 2 CNV, and was determined to show negative results. This also may represent a training curve for the photographers because the OCTA images take a longer time to acquire versus a

standard volumetric scan and may be more difficult to acquire without motion artifact. Eye-tracking software would reduce this artifact.

Furthermore, because it relies on change between 2 consecutive B-scans, OCTA detects flow only higher than a minimal threshold, the slowest detectable flow, which is determined by the time between the 2 sequential OCT B-scans. Slow-flow lesions that have flow of less than the slowest detectable flow therefore would not be visualized using this imaging technique. Increasing the time between consecutive OCT B-scans could allow for increased flow detection but would offer a trade-off of increased movement artifact.

A larger, prospective study would be ideal to confirm further the sensitivity and specificity rates of the current prototype AngioVue OCTA system reported in this study. A high specificity but low sensitivity may suggest that the existing protocol for OCTA may be a better tool for noninvasively following up CNV over time than for screening for undiagnosed CNV. A specificity of 91% obtained in this study showed that OCTA could be a useful technique to confirm the presence of CNV when other methods are equivocal. This is especially true because interpretation of FAs in a clinical setting may not be as sensitive for detection of CNV as a reading center assessment, which uses highly trained observers. In 1 of our cases, for example, when FA results were positive but difficult to assess, the clinician interpreted the FA as equivocal, but the OCTA was able to visualize the CNV (Fig 6).

Our study found a sensitivity of 0% for the detection of CNV using reflectance en face OCT. This is thought to be because the reflectance en face OCT images acquired using the current standard OCTA protocol do not use oversampling or EDI, thereby generating scans that do not have high enough resolution to evaluate accurately for CNV. An



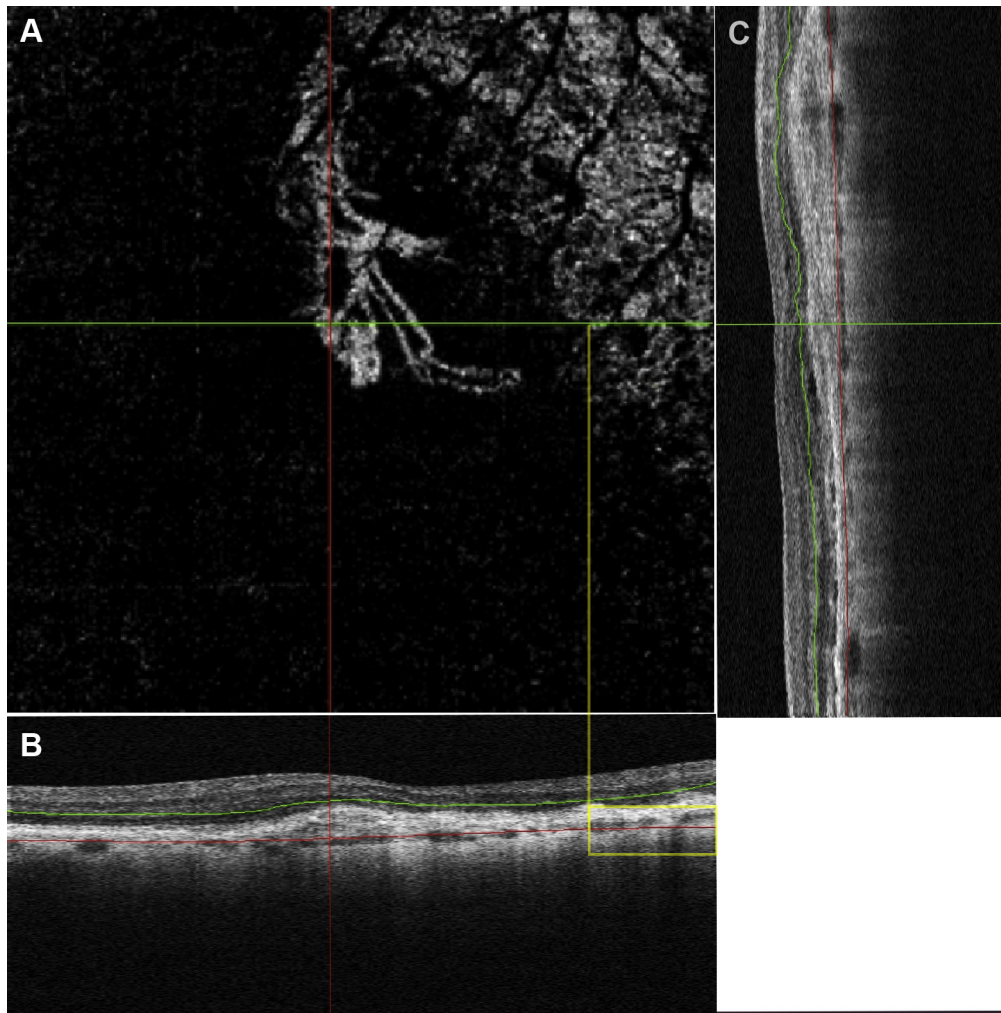


**Figure 8.** Distinguishing choroidal neovascularization (CNV) from choriocapillaris. **A**, A 3×3-mm optical coherence tomography angiography (OCTA) image of a 72-year-old white woman with neovascular age-related macular degeneration. The choriocapillaris is visualized in the top right corner and appears as a homogenous and ill-defined fine network of vessels with a granular appearance. In contrast, the CNV is discernible by its longer, thicker, more easily identifiable and more sparsely oriented vessels. **B**, Correlating y-axis optical coherence tomography (OCT) B-scan. **C**, The correlating x-axis OCT B-scan showing where the automated lower boundary erroneously includes the choriocapillaris in the OCTA image (yellow box).

important next step in the assessment of the usefulness of OCTA compared with another noninvasive technique is a study comparing OCTA with reflectance en face (EDI) OCT in type 1 CNV.

In the future, larger fields of view will be critical to evaluate more peripheral lesions, especially when screening for unknown pathologic features. Although the 3×3-mm OCTA images provided more detail of the very fine CNV vessels, the 3×3-mm and 6×6-mm OCTA images were comparable in detecting and evaluating size and general characteristics of the CNV. As OCTA image scan sizes increase to more clinically desired fields of view, it is crucial to maintain the image resolution, and thus sensitivity, of the technology. Faster scanning speeds would obtain more A-scans in each OCTA volume and therefore would output higher-resolution images at larger scanning areas.

Limitations of this study include its mostly cross-sectional nature and small sample size. In addition, segmentation to

remove choriocapillaris sometimes was not possible using the current automated prototype software because the user was unable to correct manually the shape of the automatically detected curvature lines delineating the region of interest. [Figure 8](#) illustrates this difficulty, while also demonstrating how the CNV still can be differentiated from the choriocapillaris. The choriocapillaris is a homogenous group of fine vessels that are difficult to distinguish as individual vessels, whereas CNV vessels are much more discernible as individual vascular networks. The correlating OCT B-scans show where the automatically delineated outer boundary inaccurately included the choriocapillaris superonasally. In the future, adding the ability to correct the segmentation curvature manually could facilitate further the accuracy of the AngioVue OCTA software. This would allow more complete removal of the choriocapillaris artifact from the outer retina images. Nonetheless, [Figure 8](#) demonstrates how CNV vessels appear qualitatively

different from choriocapillaris vessels even in the presence of the choriocapillaris artifact.

Additionally, although accurate segmentation of a single outer retina OCTA image without choriocapillaris was not always possible, dynamic adjustment of the segmentation boundaries was used by the readers in this study to ensure accuracy of the results. This process entailed meticulously scrolling through the OCTA images and their corresponding OCT B-scans like cube scans to pinpoint specific locations of segmentation error. These locations then were evaluated individually by adjusting the outer border to align with Bruch's membrane at each area. Therefore, the readers were able to determine the depth of the vessels. This process, although time consuming, was helpful in differentiating CNV from choroidal vessels, especially when determining the boundaries of the CNV. In a busy clinic setting, however, dynamic adjustment of the boundaries is not a feasible option. Therefore, more accurate automated segmentation and the ability to segment images manually are important future developments.

Optical coherence tomography angiography allows the clinician to visualize CNV and adjacent subretinal fluid noninvasively. Coregistration of the OCTA images with the concurrent OCT B-scans permits 3-dimensional visualization of retinal blood flow and structure in tandem. This provides a potential future method for identifying and managing CNV. The ability to detect CNV and subretinal fluid noninvasively using OCTA, as well as to visualize changes longitudinally, may lead to a decreasing necessity to rely on more invasive imaging techniques such as FA. Future studies with more varied patient demographics and larger sample sizes for higher-powered sensitivity and specificity determinations are necessary to evaluate the robustness of this technique with various types of CNV. Furthermore, a study describing the differences between clinically active and inactive CNV on OCTA are critical in evaluating further OCTA's usefulness in the clinical setting.

## References

1. Ferrara D, Mohler KJ, Waheed N, et al. En-face enhanced-depth swept-source optical coherence tomography features of chronic central serous chorioretinopathy. *Ophthalmology* 2014;121:719–26.
2. Ambati J, Ambati BK, Yoo SH, et al. Age-related macular degeneration: etiology, pathogenesis, and therapeutic strategies. *Surv Ophthalmol* 2003;48:257–93.
3. Yannuzzi LA, Negrao S, Lida T, et al. Retinal angiomatic proliferation in age-related macular degeneration. *Retina* 2001;21:416–34.
4. Jia Y, Bailey ST, Wilson DJ, et al. Quantitative optical coherence tomography angiography of choroidal neovascularization in age-related macular degeneration. *Ophthalmology* 2014;121:1435–44.
5. Do DV, Gower EW, Cassard SD, et al. Detection of new-onset choroidal neovascularization using optical coherence tomography: the AMD DOC study. *Ophthalmology* 2012;119:771–8.
6. Kotsolis AI, Killian FA, Ladas ID, Yannuzzi LA. Fluorescein angiography and optical coherence tomography concordance for choroidal neovascularization in multifocal choroiditis. *Br J Ophthalmol* 2010;94:1506–8.
7. Do DV. Detection of new-onset choroidal neovascularization. *Curr Opin Ophthalmol* 2013;24:224–7.
8. Ryan SJ, Sadda SR, Hinton DR, et al. Age-related macular degeneration. In: Ryan SJ, Sadda SR, Hinton DR, ed. *Retina* 5th ed, Vol. 1 London: Elsevier Saunders; 2013:1150–82.
9. Shah SM, Tatlipinar S, Quinlan E, et al. Dynamic and quantitative analysis of choroidal neovascularization by fluorescein angiography. *Invest Ophthalmol Vis Sci* 2006;47:5460–8.
10. Sulzbacher F, Kiss C, Munk M, et al. Diagnostic evaluation of type 2 (classic) choroidal neovascularization: optical coherence tomography, indocyanine green angiography, and fluorescein angiography. *Ophthalmology* 2011;122:799–806.
11. Kwitrovich KA, Maguire MG, Murphy RP, et al. Frequency of adverse systemic reactions after fluorescein angiography. Results of a prospective study. *Ophthalmology* 1991;98:1139–42.
12. Lopez-Saez MP, Ordoqui E, Tornero P, et al. Fluorescein-induced allergic reaction. *Ann Allergy Asthma Immunol* 1998;81:428–30.
13. Coscas F, Coscas G, Querques G, et al. En face enhanced depth imaging optical coherence tomography of fibrovascular pigment epithelium detachment. *Invest Ophthalmol Vis Sci* 2012;53:4147–51.
14. Liakopolous S, Ongchin S, Bansal A, et al. Quantitative optical coherence tomography findings in various subtypes of neovascular age-related macular degeneration. *Invest Ophthalmol Vis Sci* 2008;49:5048–54.
15. Sadda SR, Liakopolous S, Keane PA, et al. Relationship between angiographic and optical coherence tomographic (OCT) parameters for quantifying choroidal neovascular lesions. *Graefes Arch Clin Exp Ophthalmol* 2010;248:175–84.
16. Giant A, Luiselli C, Esmaili DD, et al. Spectral-domain optical coherence tomography as an indicator of fluorescein angiography leakage from choroidal neovascularization. *Retina* 2011;32:5579–86.
17. Kim DY, Finger J, Zawadzki RJ, et al. Optical imaging of the chorioretinal vasculature in the living human eye. *Proc Natl Acad Sci U S A* 2013;110:14354–9.
18. Choi W, Mohler KJ, Potsaid B, et al. Choriocapillaris and choroidal microvasculature imaging with ultrahigh speed OCT angiography. *Plos One* 2013;8:e81499.
19. Schwartz DM, Fingler J, Kim DY, et al. Phase-variance optical coherence tomography: a technique for noninvasive angiography. *Ophthalmology* 2014;121:180–7.

## Footnotes and Financial Disclosures

Originally received: December 7, 2014.

Final revision: January 18, 2015.

Accepted: January 30, 2015.

Available online: ■■■■.

Manuscript no. 2014-1963.

<sup>1</sup> New England Eye Center and Tufts Medical Center, Tufts University, Boston, Massachusetts.

<sup>2</sup> Department of Electrical Engineering and Computer Science and Research Laboratory of Electronics, Massachusetts Institute of Technology, Cambridge, Massachusetts.

<sup>3</sup> CAPES Foundation, Ministry of Education of Brazil, Brasilia, Brazil.

## Financial Disclosure(s):

The author(s) have made the following disclosure(s): J.S.D.: Consultant and financial support – Carl Zeiss Meditec, Inc. (Dublin, CA) and OptoVue, Inc. (Fremont, CA).

Supported in part by an unrestricted grant from Research to Prevent Blindness, Inc., New York, New York, to the New England Eye Center/ Department of Ophthalmology, Tufts University School of Medicine; and by the Massachusetts Lions Eye Research Fund, Inc (New Bedford, MA).

## Author Contributions:

Conception and design: de Carlo, Bonini Filho, Ferrara, Baumsal, Witkin, Duker, Waheed

Analysis and interpretation: de Carlo, Bonini Filho, Chin, Adhi, Waheed

Data collection: de Carlo, Bonini Filho, Chin, Baumsal, Witkin, Reichel, Duker, Waheed

Obtained funding: Not applicable

Overall responsibility: de Carlo, Bonini Filho, Chin, Adhi, Ferrara, Baumsal, Witkin, Reichel, Duker, Waheed

## Abbreviations and Acronyms:

**AMD** = age-related macular degeneration; **CNV** = choroidal neovascularization; **CSCR** = central serous chorioretinopathy; **EDI** = enhanced depth imaging; **FA** = fluorescein angiography; **GLD** = greatest linear dimension; **OCT** = optical coherence tomography; **OCTA** = optical coherence tomography angiography; **RPE** = retinal pigment epithelium; **RPED** = retinal pigment epithelial detachment; **SD** = spectral domain; **SS** = swept-source; **SSADA** = split-spectrum amplitude decorrelation angiography; **VEGF** = vascular endothelial growth factor.

## Correspondence:

Nadia K. Waheed, MD, MPH, New England Eye Center at Tufts Medical Center, 260 Tremont Street, Biewend Building, 9 - 11th Floor, Boston, MA 02116. E-mail: [nadiakwaheed@gmail.com](mailto:nadiakwaheed@gmail.com).